

Marked Point Identification for Interventional Operation Navigation of Digital Subtraction Angiography Image based on Triangle Topology

Boyang Wang^{1,2,*}, Bin Chen³ and Jian Wu¹

¹Research Center of Biomedical Engineering, Graduate School at Shenzhen, Tsinghua University, Shenzhen 518055, China

²Department of Biomedical Engineering, Tsinghua University, Beijing 100084, China

³Chinese Medicine Hospital, Shenzhen 518033, China

Received 9 July 2016; Accepted 28 November 2016

Abstract

Identifying the coordinates of marked points in digital subtraction angiography (DSA) is one of the key problems in DSA image-guided navigation systems for interventional radiological procedures. DSA images directly affect the precision and speed of navigation. In this work, a novel method for marked point identification was proposed on the basis of the geographical concept of triangle topology to identify the coordinates of the marked points in a DSA image rapidly and accurately. First, a calibration model with special and distributed marked points was designed. The identifiable marked points from the pretreated image were then selected and the image coordinate of the fourth marked point was verified for calibration. Subsequently, the structure of the triangle topology and proportional relation were used to confirm the uniformized coordinates of the four points. These four points were used to calculate the homography from the coordinates of the uniformized coordinate system to the coordinates of the image coordinate system. Finally, the image coordinates of all the marked points were derived through the values of the uniformized coordinates and homography. Results show that through the marked point identification method proposed in this study, the locations of the marked points can be determined accurately and quickly in the image coordinate system and uniformized coordinate system based on the triangle topology structure, which was formed by the identifiable marked points. The image coordinates of all the marked points can be recalculated without identifying the special marked points. The average error in the algorithm is smaller than 1 mm, and the running time is shorter than 1 s. These values satisfy the requirements of actual surgery in terms of the precision and speed. Thus, the proposed method can provide practical reference for future navigation system based on DSA images for interventional operation.

Keywords: DSA image, marked point identification, image-guided navigation

1. Introduction

Minimally invasive surgery is extensively used in interventional therapy because it results in less trauma, quick recovery, and good effect [1]. Transcatheter arterial chemoembolization is a treatment method for micro-traumatic intervention. In this method, a special catheter is inserted precisely into the target arteries that feed the tumor. An embolic agent of proper amount is then injected into the catheter at a proper speed to close and block the target arteries. This process eventually causes the avascular necrosis of tumor issue. During the process, the contrast agent must be injected to reveal the vascular structure in order to locate the catheter tip [2],[3]. However, this method has several disadvantages. First, radiography is necessary every time the catheter tip is located. Prolonged use of contrast agent can cause adverse effects on patients, and X-ray radiation can cause radius damage to both doctors and patients. Thus, other methods have been proposed for micro-traumatic intervention. One such method is a surgery navigation system based on digital subtraction angiography (DSA) images [4-7]. This system comprises an X-ray generator for angiography, electromagnetic tracking

equipment, and computer software platform [8],[9] and thus can display the location of the catheter tip accurately in the DSA image at real time and draw the catheter route in the anatomical structure; thus, this method not only reduces the adverse effects to the patients and doctors by decreasing the times of radiography but also provides a visual guide for doctors during surgical operations [10]. Meanwhile, in this method, installing an electromagnetic tracking sensor at the tip of the catheter is necessary to locate the catheter tip accurately. In addition, a calibration model is used. Calibration model refers to the lattice with the materials featured by low X-ray penetration rates. These materials are distributed in the board made of materials with high X-ray penetration rates. The transformation matrix is then calculated using the coordinates of the lattice in the calibration model of the DSA image coordinate system. The coordinate of the transformation matrix in the electromagnetic orientation system is also calculated. The corresponding relation between the DSA image coordinate system and the electromagnetic positioning coordinate system during the transformation of the three-dimensional location of the catheter tip into the two-dimensional DSA image is used for matrix calculation. Thus, this method provides visual guidance for doctors during catheter operation of the doctor. In this regard, accurately locating the lattice of the calibration model in the DSA image is

* E-mail address: wby14@mails.tsinghua.edu.cn

crucial to attain high precision. Despite the importance of this process, it remains a critical problem of surgery navigation based on DSA images.

In this study, a method based on triangle topology for the automatic identification of the marked point of a DSA image is proposed. It can reconstruct the image coordinate of all the marked points by using the marked points with identifiable parts. Reconstruction is performed to locate the lattice of the model in the DSA image coordinate system accurately and quickly. The proposed method can lay foundations for surgery navigation systems based on DSA images.

2. State of the art

Many solutions have been proposed to solve the problem of marked point identification in DSA images. The identification process can be divided into two methods, that is, online and offline. In offline calibration methods, marked point identification is performed for the specific angle of the C-arm and focal length before the surgery. However, while offline calibration is highly précised, it requires additional calibration processes before the surgery. Thus, the burden on the operator increases, and the surgery becomes rather complicated. Moreover, only the specific locations of the C-arm can be selected for marked point identification. Thus, the application of identification is limited. Online calibration refers to the real-time calibration during surgery. It can determine the image coordinate and the location coordinate and break the limitations of offline calibration with regard to the locations of the C-arm. In this round template image with the same size as the marked point and the pretreated reference image for correlation calculation are selected by using the normalized cross-correlation ideas in classical statistic matching; this procedure is performed by calculating the cross-correlation metric value regardless of whether the area that contains the pixels of the marked point can be determined [11]. In this method, the image of the round template must be determined first. When the C-arm translates along the imaging principal axis, its size in the image changes after the imaging of the marked point. However, the predetermined template image might become invalid and thus may cause identification failure. During the calculation of mutual information, threshold value selection presents a problem, which cannot be determined unless a numerous experiments and tests are performed [11–16]. Li et al. [10] proposed the use of clustering algorithm for the automatic identification of information on the mark points and determination of the grid posture of the marked points through the table of row/column index. In the clustering process, the calculation may be affected by the noise points in the image. If a contrast agent is present in the image, the identification may fail. Meanwhile, the method has adopted the clustering concepts of the minimum spanning tree. However, its application is quite complicated. This method involves many calculations when the clustering calculation is performed, and thus its real-time performance cannot satisfy the requirement of fast calibration during the surgery. Si et al. [17] proposed a method that identifies the image coordinate of a marked point according to the simple ratio. Although this method is quite simple, special marked point must be correctly identified, especially for those images with contrast agent “pollution” or viewport changes. Notably, the identification fails when the special marked point is not identified. Thus, an automatic identification method for the marked point of DSA image is proposed in this study to

address the problems on marked point identification methods in terms of feasibility, correctness, and real-time performance. This method can determine the image coordinate of a marked point accurately and quickly.

The rest of this paper is organized as follows. The construction of a surgery navigation system based on the DSA image is elaborated and the requirement of catheter calibration is raised in the third section. A new marked point identification method is then proposed. In the fourth section, an experiment is conducted to verify the effectiveness, correctness, and real-time performance of the algorithm of the marked point identification. The experiment results are then analyzed. In the last section, the conclusion and expectations are provided.

3. Methodology

3.1 Surgery navigation system design based on DSA images

Surgery navigation system based on DSA images is composed of angiography X-ray generator, calibration model, the electromagnetic positioning device, and the catheter with electromagnetic sensor. The software used to run the system contains a 3D slicer software platform. Figure 1 shows the navigation process. The standard coordinate system is as follows:

- EMT* —electromagnetic tracking coordinate
- DSA* —DSA imaging system coordinate
- Image* —DSA image coordinate.

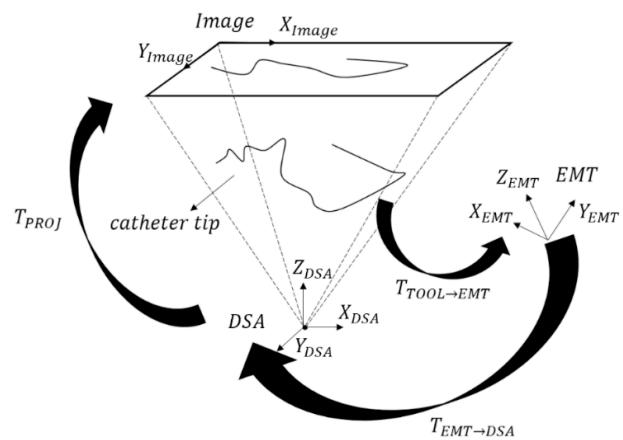


Fig. 1. Process of catheter calibration

The coordinate of the catheter tip in the DSA imaging system is obtained by using the locations of the catheter tip in the electromagnetic tracking coordinate system $T_{TOOL \rightarrow EMT}$ and through the transformation $T_{EMT \rightarrow DSA}$ from the electromagnetic tracking coordinate system to the DSA imaging coordinate system. Subsequently, the coordinate of the catheter tip in the DSA image can be used through the projection T_{PROJ} for the real-time display of the catheter tip in the DSA image. The real-time display facilitates the tracing of the route of the catheter in the blood vessel. This Thus, it can assist doctors performing the intubation.

Calibrating the catheter is necessary to complete the procedure chart. The Aurora electromagnetic tracking device developed by NDI company is used to obtain $T_{TOOL \rightarrow EMT}$ of the catheter tip in the electromagnetic tracking coordinate system. T_{PROJ} is calculated according to the projection relations in the DSA coordinate system. Assuming that the

distance from the radioactive source to the imaging planes is f , then

$$X_{image} = f \frac{X_{DSA}}{Z_{DSA}} \quad (1)$$

and

$$Y_{image} = f \frac{Y_{DSA}}{Z_{DSA}} \quad (2)$$

Therefore, calculating the transformation of $T_{EMT \rightarrow DSA}$ during calibration is suffice. The calibration model is necessary for the calculation of $T_{EMT \rightarrow DSA}$. It can be transformed into the Perspective-n-Point problem [18] for calculation by acquiring the image coordinate and the electromagnetic tracking coordinate of the marked point in the calibration model and the focal length.

The calibration model is composed of a shell and a calibration board as shown in Figure 2. The shell is made of acrylonitrile butadiene styrene copolymers with high X-ray penetration rate. The shell is used to fix the calibration board to the flat panel detector. The calibration board can be divided into an upper layer and lower layer. Each layer is made of polymethyl methacrylate and has regularly distributed lead points with low X-ray penetration rates in the surface. The lattice is arranged with uniform spaces, as shown in Figure 3. The board of the upper layer adopts the 7 x 7 lattice, in which a single cell constitutes a large marked point with a diameter of 4 mm. The rest of cells are small marked points with a diameter of 2 mm. The cell that contain the large marked point are considered as the coordinate axis of the uniformized coordinate system. In this system, the origin of the coordinates is set as 0, as shown in Figure 3. The board of the lower layer is an 8 x 8 lattice, which contains all the small marked points with a diameter of 2 mm. The marked points are distributed among the marked points of the upper, middle, and lower layers in a two-dimensional image.

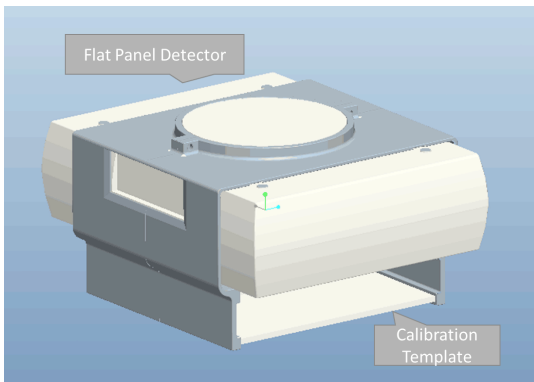


Fig. 2. Calibration model

3.2 Method for the automatic identification of marked point of DSA image according to the triangle topology
 During the acquisition of the image coordinate of the marked points in the calibration model, accuracy and speed directly affect the precision and real-time performance of the entire navigation system. Thus, a method that can automatically identify the marked point of the DSA image according to the triangle topology is proposed. This method can locate the marked points accurately and quickly.

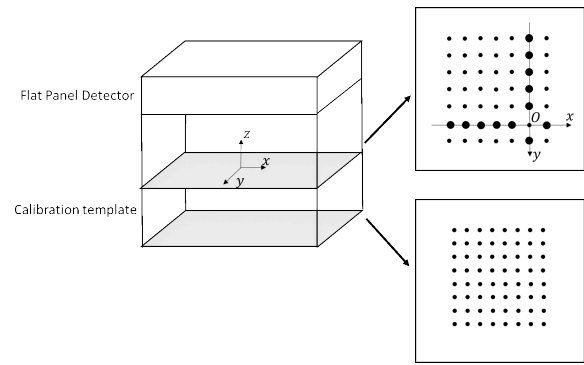


Fig. 3. Schematic diagram of marked point distribution in the calibration board

3.2.1 Pretreatment

The threshold value is selected according to the gray information obtained from the DSA image. The marked points as targets are ensured to be separated from the background. The background is removed when the marked point is extracted. For the materials and human tissue with high X-ray penetration rate, the gray value in the DSA image is relatively large. By contrast, in the contrast agent and marked point with relatively low X-ray penetration rate, the gray values in the DSA image are relatively small. The part with relatively high X-ray penetration rate and the part with relatively low X-ray penetration rate can be differentiated. In each marked point production, the amount of lead used is not consistent. The contrast agents contain different concentrations. Thus, the gray value of the contrast agent in the DSA image might be larger or smaller than the gray value of the marked point. As a result, some marked points whose gray values are larger than the contrast agent are often lost when the threshold value is used to remove the influence of the contrast agent from the part with relatively low X-ray penetration rate. Meanwhile, parts of the marked points might be present in the visual field because of the vision adjustment during the interventional operation. After the threshold value processing, some of the marked points are extracted from the DSA image.

Morphological processing is performed with threshold processing for the DSA two-value image. Each of the eight connecting components is marked in the two-value images. The resulting marks are regarded as the connected regions. The center of mass (i.e., the mean value of rows and columns of the pixels in the areas) and the area (number of pixels in the area) of each connecting component are calculated and subsequently regarded as the center of mass and the area of the marked point, respectively.

3.2.2 Extraction of the marked point

Homography is a projected mapping matrix from one plane to another plane and indicates that a corresponding relation is established between the points of two planes. Four marked points in the plane are required to calculate the homography from the uniformized coordinate system to the image coordinate system and obtain the corresponding relation between them. Moreover, at least three of the marked points must not be collinear. The marked points are arranged at a descending order. Three marked points with the largest areas are then selected, because only some parts of the marked points can be identified according to the area size calculated in the pretreatment for all the extracted marked points. The three marked points are designated as A, B, and C. According to the triangle topology, the absolute positions of

A, B, and C can be determined. The detailed determination basis is as follows:

- (1) Three points of A, B, and C are not collinear.
- (2) A and B are in the same row or column;

(3) C is not in the same row or column with the A or B.

For example, A and B can be considered in the same row with specific position of C. All the triangle topologies that the three points of A, B, and C might constitute are shown as follows:

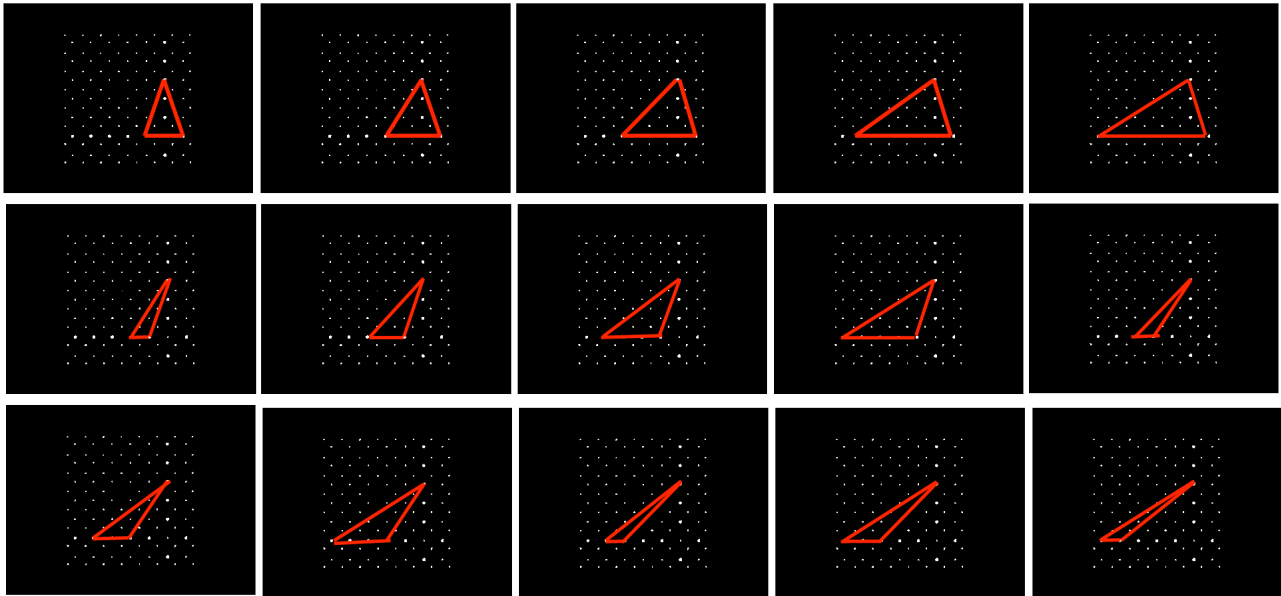


Fig. 4. Triangle topologies

Figure 4 shows some of the triangle topologies generated by A and B, which remain in the same row despite the changes in position, and C, which has a specific position.

Another point, designated as D, is used, because the establishment of homography involves four points. For point D, the other coordinate value acts as the coordinate value of point D in the corresponding locations among the two coordinate values of point A except the coordinate value similar to point B. Another coordinate value of point D is identical with the coordinate value of the corresponding location of point C. The determination method for the origin of coordinate 0 of the uniformized coordinate system is similar to point D. Among the two coordinate values of point A, the coordinate value similar to point B acts as the coordinate value of point 0 in the corresponding location. In addition, another coordinate value of point 0 is identical with the coordinate value of point C in the corresponding location.

In the image coordinate system, the above method can be used to determine the image coordinates of points 0 and D. For example, in Figure 5, A and B are in the same row. The row coordinate of point 0 is thus similar to that of point A, and the column coordinate is similar to that of point C. negative when points A and B are in the same column or positive when points A and B are not in the same column. Meanwhile, in Figure 5, when points A and B are in the same row, the symbol is negative when the number of columns of point C is smaller than the number of columns of point A. Furthermore, if the two coordinate values of point C are 0 and 3, the coordinate of point C is (0, -3). The determination method of point D in the uniformized coordinate system is similar to that in the image coordinate system. Thus, the coordinates of the four marked points in the uniformized coordinate system can be completely confirmed.

Moreover, the column coordinate of point D is the same as that of point A. The row coordinate of point D is same as that of point C. Therefore, the coordinates of points 0 and D can be determined. In addition, three of the four points are not collinear, indicating that the result satisfies the calculation requirement of homography.

In the uniformized coordinate system, the OA to OB ratio can be used to determine the uniformized coordinate system of A and B on the basis of the concepts of the simple ratio [17]. The mapping relation is shown in Table 1. According to the uniformized coordinate system of A and B, the length of unit length 1 of the uniformized coordinates in the image coordinate system is $uint=(OA+OB)/(|A|+|B|)$. The uniformized coordinate of C can be determined by using this length. In this coordinate, one coordinate value is 0 and the other coordinate value is regarded as $c=OC/uint$. The symbol is determined according to the relative relation of C with A. When the number of rows of point C is smaller than the number of rows of point A, the symbol is negative when A and B are in the same row or positive when A and B are not in the same row. When the number of columns of point C is smaller than the number of columns of point A the symbol is

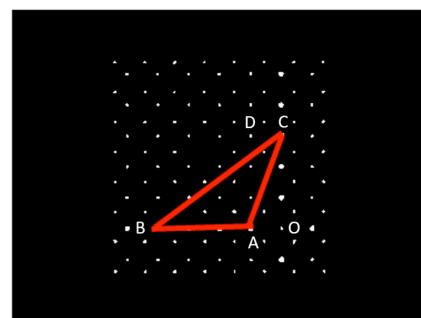


Fig. 5. Marked point identification

3.2.3 Homography and the image coordinate calculation

According to the uniformized coordinates and image coordinates of points of A, B, C, and D, the homography H from the uniformized coordinates to the image coordinate system can be calculated.

$$H = \begin{bmatrix} h_{11} & h_{12} & h_{13} \\ h_{21} & h_{22} & h_{23} \\ h_{31} & h_{32} & 1 \end{bmatrix} \quad (3)$$

Table 1. Mapping relation between the OA/OB ratio with the uniformized coordinates

Position		OA:OB	A	B	Position		OA:OB	A	B
Same Column	Different Sides	1:1	(1,0)	(-1,0)	Same Row	Different Sides	1:1	(0,1)	(0,-1)
		1:2	(1,0)	(-2,0)			1:2	(0,1)	(0,-2)
		1:3	(1,0)	(-3,0)			1:3	(0,1)	(0,-3)
		1:4	(1,0)	(-4,0)			1:4	(0,1)	(0,-4)
		1:5	(1,0)	(-5,0)			1:5	(0,1)	(0,-5)
	Same Sides	1:2	(-1,0)	(-2,0)		Same Sides	1:2	(0,-1)	(0,-2)
		1:3	(-1,0)	(-3,0)			1:3	(0,-1)	(0,-3)
		1:4	(-1,0)	(-4,0)			1:4	(0,-1)	(0,-4)
		1:5	(-1,0)	(-5,0)			1:5	(0,-1)	(0,-5)
		2:3	(-2,0)	(-3,0)			2:3	(0,-2)	(0,-3)
2:4	(-2,0)	(-4,0)	2:4	(0,-2)	(0,-4)				
2:5	(-2,0)	(-5,0)	2:5	(0,-2)	(0,-5)				
3:4	(-3,0)	(-4,0)	3:4	(0,-3)	(0,-4)				
3:5	(-3,0)	(-5,0)	3:5	(0,-3)	(0,-5)				
4:5	(-4,0)	(-5,0)	4:5	(0,-4)	(0,-5)				

Assuming that the uniformized coordinates of a point is (x_1, y_1) , the corresponding homogeneous coordinates is $(x_1, y_1, 1)$, and the image coordinate is (x_2, y_2) , the corresponding homogeneous coordinates is $(x_2, y_2, 1)$, then

$$Ah = v \quad (4)$$

where

$$A = \begin{bmatrix} x_1 & y_1 & 1 & 0 & 0 & -x_1x_2 & -x_2y_1 \\ 0 & 0 & 0 & x_1 & y_1 & 1 & -x_1y_2 & -y_1y_2 \end{bmatrix} \quad (5)$$

$$h = [h_{11} \ h_{12} \ h_{13} \ h_{21} \ h_{22} \ h_{23} \ h_{31} \ h_{32}]^T \quad (6)$$

and

$$v = [x_2 \ y_2 \ 1]^T \quad (7)$$

The coordinates of points A, B, C, and D in the image coordinate system are $A(x_A, y_A, 1)$, $B(x_B, y_B, 1)$, $C(x_C, y_C, 1)$, $D(x_D, y_D, 1)$. In addition, their coordinates in the uniformized coordinate system are $A'(x_{A'}, y_{A'}, 1)$, $B'(x_{B'}, y_{B'}, 1)$, $C'(x_{C'}, y_{C'}, 1)$, and $D'(x_{D'}, y_{D'}, 1)$. H can be determined by using the eight equations and solving unknown numbers.

The image coordinates of all the marked points can be determined by multiplying the uniformized coordinates of the discrete lattice with H . Therefore, even if the image coordinates of the marked points in image identification are lost, they can be determined through the above method.

4. Result analysis and discussion

We have conducted tests and experiments to verify the effectiveness, correctness, and real-time performance of the algorithm. In the experiment, DSA imaging system, calibration model, and graphic workstation (Dell Precision T5600 (Xeon E5-2603/8 GB/250 GB) are used. The medical data adopted is intranperative DICOM images from the invasive technology department of Shenzhen Hospital of

Traditional Chinese Medicine, with a resolution ratio of 1024 x 1024.

The image of normotopia C-arm is selected for further examinations. Matlab 8.6 is used for algorithm verification. The obtained results are shown in Figures 6, 7, and 8. The DSA image is affected by the viewport adjustment and contrast agent pollution (Figures 6, 7, and 8). On the one hand, the number of identification points is lost when the binarization processing is used to identify the marked point and remove the influence of the contrast agent (Figure 6[b]). On the other hand, the number of identification points is limited because of the viewport. The lost points can be recalculated by using the identification method based on triangle topology and identified marked points. The marked point of the board of the upper layer is selected for instructions. The results of the calculation are shown in Figures 6(c), 7(c), and 8(c), where * refers to the points obtained after the identification calculation. Apparently, the identification points after the calculation can fit the locations of marked point effectively.

Precision is the key factor of navigation systems. For the above method, the precision of the marked point identification must be verified. Only 13 typical points from Figure 6(a) are selected for analysis because of the numerous marked points. As shown in Table 2, the average error of calculation is 1.4220 pixels. The standard deviation is 1.6163 pixels. The physical coordinate of every pixel is 0.3730 mm. The average error of calculation is 0.5304 mm. The standard deviation is 0.6029 mm. In literature [10], the average error obtained through calculation is 0.92 mm by using the algorithm. Meanwhile in literature [11], the average error obtained through the algorithm is 0.70 mm. Thus, high precision can be achieved when the method discussed in the present study is used.

Real-time performance is one of the important aspects of surgery navigation. The speed of marked point identification and determination directly affects the efficiency of a surgical operation. The marked point identification is performed on images on Figures 6, 7, and 8. The running time of the algorithm is shown as Table 3 and is based on the Matlab 8.6 platform. The running time is limited within 1 s. This value is capable of fast automatic identification, and thus it satisfies the requirements of surgery navigation.

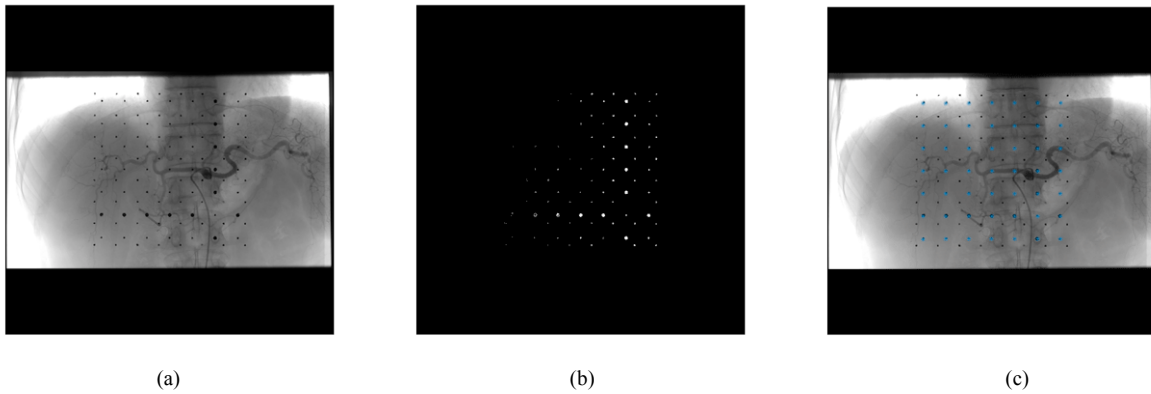


Fig. 6. Results of marked point identification of image with contrast agent pollution: (a) DSA image, (b) marked point identification before calculation, and (c) identification results after calculation

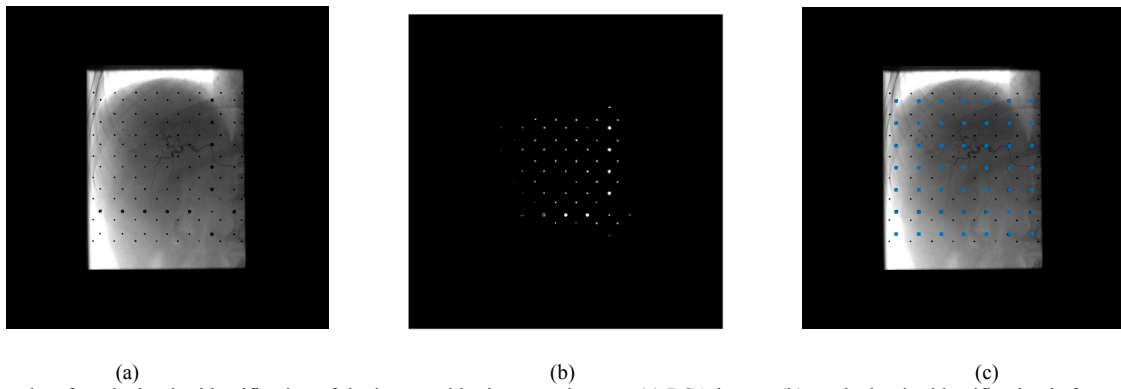


Fig. 7. Results of marked point identification of the image with viewport changes: (a) DSA image, (b) marked point identification before calculation, and (c) identification results after calculation

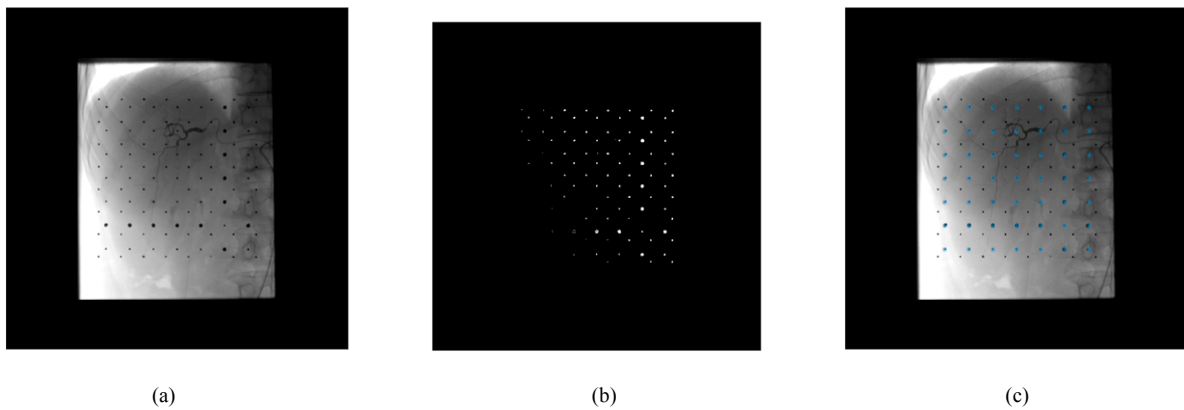


Fig. 8. Results of marked point identification with both contrast agent pollution and viewport changes: (a) DSA image, (b) marked point identification before calculation, and (c) identification results after calculation

Table 2. Experiment data of the algorithm

Marked Points	Calculation	Image Coordinate		Error (pixel)	Error(mm)
		X(pixel)	Y(pixel)		
1	before	441	303	5.3759	2.0052
	after	441.9	297.7		
2	before	653	372	0.9487	0.3539
	after	653.9	372.3		
3	before	652.7	441.7	1.7029	0.6352
	after	653.8	440.4		
4	before	653.3	512.8	1.0770	0.4017
	after	653.7	511.8		
5	before	653.6	583.3	0.5099	0.1902
	after	653.7	583.8		
6	before	653.5	654.1	0.5099	0.1902
	after	653.6	654.6		
7	before	721.4	654.1	2.9428	1.0977
	after	724.3	654.6		
8	before	582.9	654.4	0.2000	0.0746
	after	582.9	654.6		
9	before	512.1	654.5	0.2236	0.0834

	after	512.2	654.7		
10	before	441.6	654.5	0.2236	0.0834
	after	441.5	654.7		
11	before	370.7	655	0.2236	0.0834
	after	370.8	654.8		
12	before	303.2	655.2	3.1257	1.1659
	after	300.1	654.8		

Table 3. Running time of algorithm

Experiment	Running time(s)
1	0.787
2	0.803
3	0.764

5 Conclusion

A new algorithm for the automatic identification of marked point is proposed to address the problems with regard to feasibility, correctness, and speed of automatic identification of marked points in surgery navigation based on DSA images. The algorithm is proposed to calculate the image coordinates of all the marked points according to identifiable marked points. The threshold values are segmented to determine the area and center of the marked point. The area and center are determined on the basis of the locations of uniformized coordinates determined by the identified marked point. The transformational relation is then calculated to solve the image coordinates of all the marked points. Based on the experiment results, the following conclusions are obtained:

1) The coordinates of the identifiable marked point in the uniformized coordinate system based on the triangle topology are determined. The image coordinate system can

be matched with the uniformized coordinate system simply and quickly when constructing the homography.

2) The image coordinates of all the marked points can be determined through the homography based on the uniformized coordinates of known marked points. The calculation error is minimal. This result is not the main source of error. Moreover, the outcome satisfies the demands of surgery navigation system.

3) For the lost marked point in the identification, the uniformized coordinates and homography can be used to perform recovery calculation. Moreover, identifying a special marked point is unnecessary. Thus, the proposed method is highly flexible.

The method is simple and feasible, because the image calculation for automatic identification and extraction of marked point are realized. In addition, it can calculate the image coordinate quickly, thus increasing its flexibility. Furthermore, its precision satisfies the requirement of interventional operation navigation. Thus, the proposed method can lay solid foundation for the establishment of surgery navigation system. Meanwhile, identification algorithm must be included in the system for analysis in subsequent studies because the entire navigation system remains underdeveloped. Doing so can perfect the precision and real-time performance analysis.

References

- Ambrosini, P., Smal, I., Ruijters D., Niessen, W. J., Moelker, A., Walsum, T. V., "3D Catheter Tip Tracking in 2D X-ray Image Sequences Using a Hidden Markov Model and 3D Rotational Angiography". *Lecture Notes in Computer Science*, 9365, 2015, pp.38-49.
- Ambrosini, P., Ruijters, D., Moelker, A., Niessen, W. J., Walsum, T. V., "2D/3D Catheter-Based Registration for Image Guidance in TACE of Liver Tumors". *Information Processing in Computer-Assisted Interventions*, 2014, pp.246-255.
- Ambrosini, P., Ruijters, D., Niessen, W. J., Moelker, A., Walsum, T. V., "Continuous roadmapping in liver TACE procedures using 2D-3D catheter-based registration". *International Journal of Computer Assisted Radiology and Surgery*, 10(9), 2015, pp. 1357-1370.
- Sati, M., Stäubli, H. U., Bourquin, Y., Kunz, M., Käsermann, S., Nolte, L. P., "Clinical integration of computer-assisted technology for arthroscopic anterior cruciate ligament reconstruction". *Operative techniques in orthopaedics*, 10(1), 2000, pp.40-49.
- Liu, W., Wang, M., Wang, T., "Error analysis of a computer-assisted orthopedic system for distal locking of intramedullary nail". *Journal of Beijing University of Aeronautics and Astronautics*, 30(9), 2004, pp.850-854.
- Huang, H. F., Zhang P., "Automated Correction for the Distortion of Digital Subtracted Angiography Image based on Morphology and Polynomial". *Journal of Biomedical Engineering Research*, 27(1), 2008, pp.31-35.
- Sati, M., Stäubli, H. U., Bourquin, Y., Kunz, M., Nolte, P. L., "Real-time computerized in situ guidance system for ACL graft placement". *Computer Assisted Surgery*, 7(1), 2002, pp.25-40.
- Cleary, K., Peters, T. M., "Image-Guided Interventions: Technology Review and Clinical Applications". *Annual review of Biomedical Engineering*, 12(12), 2010, pp.119-142.
- Peters, T. M., "Image-guidance for surgical procedures". *Physics in Medicine & Biology*, 51 (14), 2006, pp.505-540.
- Qian, L. W., Wang, C. T., Yan S. J., Xia, Q., "Automatic Calibration Method for C-arm Camera Model Based on Calibration Target". *Computer Engineering*, 35(15), 2009, pp.7-12.
- Livyatan, H., Yaniv, Z., Joskowicz, L., "Robust automatic C-arm calibration forfluoroscopy-based navigation: a practical approach". *Lecture Notes in Computer Science*, 2489, 2002, pp. 60-68.
- Markelj, P., Tomaževič, D., Likar, B., Pernuš, F., "Review of 3D/2D registration methods for image-guided interventions". *Medical Image Analysis*, 16(3), 2012, pp.642-661.
- Yang, C. D., Chen, Y. W., Tseng, C. S., Ho, H. J., "Non-invasive, fluoroscopy-based, image-guided surgery reduces radiation exposure for vertebral compression fractures: A preliminary survey". *Formosan Journal of Surgery*, 45(1), 2012, pp.12-19.
- Liang, J. T., Doke, T., Onogi, S., "Fluorolaser navigation system to guide linear surgical tool insertion". *International Journal of Computer Assisted Radiology and Surgery*, 7(6), 2012, pp.931-939.
- Ren, H., "Computer-assisted bone tumour ablation using sparse radiographs". *Advanced Robotics*, 28(5), 2014, pp.303-315.
- Tersi, L., Stagni, R., Tersi, L., Stagni, R., "Effect of calibration error on bone tracking accuracy with fluoroscopy". *Journal of Biomechanical Engineering*, 136(5), 2014, pp.324-337.
- Meng, C., Zhang, J., Lv S. J., "Automatic Matching Technology for C-arm Image Marked Points Based on Simple Ratio". *Chinese Journal of Biomedical Engineering*, 29(5), 2010, pp.654-659.
- Zhou, H. Y., Zhang, T., Lu, W. N., "Vision-based pose estimation from points with unknown correspondences". *IEEE Transactions on Image Processing*, 23(8), 2014, pp.3468-3477.